

---

# REPRESENTATION OF THE STRUCTURE OF GRAPHS BY SEQUENCES OF INSTRUCTIONS

---

A PREPRINT

 **Ezequiel López-Rubio\***

Department of Computer Languages and Computer Science  
 University of Málaga  
 Bulevar Louis Pasteur, 35  
 29071 Málaga, Spain  
 ezeqlr@lcc.uma.es

December 16, 2025

## ABSTRACT

The representation of graphs is commonly based on the adjacency matrix concept. This formulation is the foundation of most algebraic and computational approaches to graph processing. The advent of deep learning language models offers a wide range of powerful computational models that are specialized in the processing of text. However, current procedures to represent graphs are not amenable to processing by these models. In this work, a new method to represent graphs is proposed. It represents the adjacency matrix of a graph by a string of simple instructions. The instructions build the adjacency matrix step by step. The transformation is reversible, i.e., given a graph the string can be produced and vice versa. The proposed representation is compact, and it maintains the local structural patterns of the graph. Therefore, it is envisaged that it could be useful to boost the processing of graphs by deep learning models. A tentative computational experiment is reported, demonstrating improved classification performance and faster computation times with the proposed representation.

**Keywords** graph representation · adjacency matrix · instruction sequences · deep learning · language models · structural patterns

## 1 Introduction

Graphs provide a flexible abstraction for relational data in domains such as social networks, molecules, knowledge graphs, recommendation, and databases [Zhou et al., 2020, Khoshrafter and An, 2024, Ju et al., 2024]. The standard approach to graph processing with deep learning models is to learn a suitable representation of them. The goal of graph representation learning is to map nodes, edges, subgraphs, or whole graphs into low-dimensional vectors that preserve structural properties and attributes, enabling downstream tasks such as node classification, link prediction, graph classification, and anomaly detection [Khoshrafter and An, 2024, Ju et al., 2024].

Early work on graph representation focused on *shallow* embedding methods that learn a lookup table of node embeddings optimized for proximity in the original graph [Khoshrafter and An, 2024]. Random-walk-based methods such as DeepWalk and node2vec treat truncated random walks as sentences and apply word embedding techniques to enforce that co-visited nodes obtain similar vectors [Perozzi et al., 2014, Grover and Leskovec, 2016]. Matrix factorization approaches, including Laplacian eigenmaps and variants based on factorizing pointwise mutual information matrices, can be interpreted as implicitly optimizing similar proximity objectives [Belkin and Niyogi, 2003, Ou et al., 2016]. These techniques are scalable and effective but decouple representation learning from node features and struggle to generalize to unseen nodes or dynamic graphs [Khoshrafter and An, 2024, Ju et al., 2024].

---

\*Corresponding author. ITIS Software. Universidad de Málaga. C/ Arquitecto Francisco Peñalosa 18, 29010, Málaga, Spain

Extensions of shallow embeddings incorporate side information and edge types, e.g., for heterogeneous and knowledge graphs. Knowledge graph embedding methods such as TransE, DistMult, and RotatE embed entities and relations into continuous spaces and define scoring functions for triplets [Wang et al., 2017]. While powerful for link prediction, these models typically ignore higher-order structure and are limited in expressivity compared to modern deep architectures [Wang et al., 2017, Ju et al., 2024].

Deep graph representation learning is now dominated by Graph Neural Networks (GNNs), which implement message passing over the graph structure [Zhou et al., 2020, Wu et al., 2021]. In the standard message-passing framework, each node iteratively aggregates information from its neighbors and updates its hidden state using a permutation-invariant function, yielding embeddings that combine local structure and node features [Gilmer et al., 2017, Zhou et al., 2020]. Popular instances include Graph Convolutional Networks (GCN), GraphSAGE, and Graph Attention Networks (GAT), which differ mainly in their neighborhood aggregation and normalization schemes [Kipf and Welling, 2017, Hamilton et al., 2017, Veličković et al., 2018].

GNNs can be categorized by their architectural principles [Zhou et al., 2020, Ju et al., 2024]. Spectral GNNs define convolutions via the graph Laplacian eigenbasis, while spatial GNNs perform aggregation directly in the vertex domain using learned filters [Bruna et al., 2014, Kipf and Welling, 2017]. Recurrent and attention-based variants replace simple aggregators with recurrent units or attention mechanisms to capture more expressive interactions [Gilmer et al., 2017, Veličković et al., 2018]. Recent work connects GNN expressivity to the Weisfeiler–Lehman (WL) test, leading to architectures such as Graph Isomorphism Networks (GIN) that match the discriminative power of the 1-WL test under certain conditions [Xu et al., 2019].

In this work, a completely different approach is taken. Rather than learning a representation, a new, fixed way to represent graphs is proposed. The approach is based on representing the adjacency matrix of the graph by a string of simple instructions. Our overall goal is to design a graph representation methodology that is amenable to processing by deep language models.

The structure of this paper is as follows. Section 2 presents the graph representation methodology. After that, Section 3 reports the results of an exploratory computational experiment. Finally, Section 4 deals with the conclusions.

## 2 Methodology

In this section, the proposed methodology to represent the structure of a graph is detailed. Let  $G = (V, A)$  be a graph where  $V = \{v_1, \dots, v_N\}$  is the set of vertices, and  $A$  is the set of edges  $(v_i, v_j)$ , with  $v_i, v_j \in V$ . It will be assumed that a complete order is defined on the  $N$  elements (vertices) in  $V$ , i.e.,  $v_1$  is the first vertex, up to the last vertex  $v_N$ . Then, the adjacency matrix associated with  $G$  will be noted  $M_G$ , which has  $N \times N$  elements:

$$M_G(i, j) = \begin{cases} 0 & \text{if } (v_i, v_j) \in A \\ 1 & \text{if } (v_i, v_j) \notin A \end{cases} \quad (1)$$

The adjacency matrix  $M_G$  is symmetric for undirected graphs, while it may not be symmetric for directed graphs. It comprises the structure of the graph  $G$ . A standard way to represent such a structure by a string is to flatten the adjacency matrix into a binary string row by row:

$$B_G = M_G(1, 1) \dots M_G(1, N) \ M_G(2, 1) \dots M_G(N, N) \quad (2)$$

where  $B_G \in \{0, 1\}^*$  is a string of  $N^2$  symbols.

### 2.1 String representation

Next, an alternative method to represent the structure of  $G$  is given. A string  $w \in \{U, D, L, R, E\}^*$  is associated with  $G$ , where the five possible symbols are interpreted as instructions that can be executed to build  $M_G$  starting from the null matrix of size  $N \times N$ . A pointer  $\mathbf{p} = (p_1, p_2) \in \{1, \dots, N\} \times \{1, \dots, N\}$  to an element of  $M_G$  will be maintained, which starts at position  $(1, 1)$ . The string  $w$  is executed symbol by symbol, from left to right. The current and next values of the pointer are noted  $\mathbf{p}$  and  $\mathbf{p}'$ , while the current and next values of the adjacency matrix are noted  $M$  and  $M'$ , respectively. The semantics (meaning) of the instructions are:

- $U$  moves the pointer up if possible:

$$\mathbf{p}' = \begin{cases} \mathbf{p} & \text{if } p_1 = 1 \\ (p_1 - 1, p_2) & \text{if } p_1 > 1 \end{cases} \quad (3)$$

- $D$  moves the pointer down if possible:

$$\mathbf{p}' = \begin{cases} \mathbf{p} & \text{if } p_1 = N \\ (p_1 + 1, p_2) & \text{if } p_1 < N \end{cases} \quad (4)$$

- $L$  moves the pointer left if possible:

$$\mathbf{p}' = \begin{cases} \mathbf{p} & \text{if } p_2 = 1 \\ (p_1, p_2 - 1) & \text{if } p_2 > 1 \end{cases} \quad (5)$$

- $R$  moves the pointer right if possible:

$$\mathbf{p}' = \begin{cases} \mathbf{p} & \text{if } p_2 = N \\ (p_1, p_2 + 1) & \text{if } p_2 < N \end{cases} \quad (6)$$

- $E$  inserts a new edge at the pointer position:

$$M'(i, j) = \begin{cases} 1 & \text{if } (i = p_1) \wedge (j = p_2) \\ M(i, j) & \text{if } (i \neq p_1) \vee (j \neq p_2) \end{cases} \quad (7)$$

where the element  $M'(j, i)$  is also set to 1 if  $G$  is defined as an undirected graph.

The execution of any string in  $\{U, D, L, R, E\}^*$  produces an adjacency matrix. In other words, the set of valid strings is the regular language  $\{U, D, L, R, E\}^*$ . Conversely, given an adjacency matrix, there are infinite strings  $w \in \{U, D, L, R, E\}^*$  that can produce it. For example, one can add pointer movement instructions that cancel each other. In order to have a canonical string to represent each graph, an algorithm is provided. The algorithm accepts an adjacency matrix  $M$  as input, produces a string  $w \in \{U, D, L, R, E\}^*$  as output, and keeps a local variable  $\mathbf{p}$  that is a pointer to an element of  $M$ .

1. Initialize the pointer  $\mathbf{p}$  to  $(1, 1)$ , i.e the upper left corner of  $M$ .
2. Initialize  $w$  to the empty string.
3. If  $M$  is null then halt and return  $w$ . Otherwise, go to step 4.
4. Find the nonzero cell  $\mathbf{q} \in \{1, \dots, N\} \times \{1, \dots, N\}$  of  $M$  which is closest to  $\mathbf{p}$  according to Manhattan distance. If there is more than one closest nonzero cells, then choose the cell for which the difference  $q_1 - p_1$  is smallest.
5. Append  $U$  or  $D$  instructions to  $w$  as required to move the pointer  $\mathbf{p}$  to the same row as  $\mathbf{q}$ .
6. Append  $L$  or  $R$  instructions to  $w$  as required to move the pointer  $\mathbf{p}$  to the same column as  $\mathbf{q}$ .
7. Append instruction  $E$  to  $w$ .
8. Set the element of  $M$  pointed by  $\mathbf{p}$  to zero. If  $G$  is undirected, then set its symmetric element to zero too.
9. Go to step 3.

The above algorithm follows a greedy approach to find short substrings of pointer movement instructions so that the overall length of the canonical representation of the input graph is kept small. There is no guarantee that this is the shortest possible string to represent  $G$ , but it is guaranteed that for each graph  $G$  there is a unique canonical string that represents it, namely the output of the above algorithm. Let us note  $I_G \in \{U, D, L, R, E\}^*$  the canonical string for graph  $G$ .

## 2.2 Representation length

The length of the canonical string is upper bounded by  $2N^2 - 1$ . The worst case is an adjacency matrix of a complete directed graph, i.e. all elements of the matrix are one. In this case, each element requires one pointer movement instruction plus one  $E$  instruction except the first element  $(1, 1)$ , which only needs an  $E$  instruction.

Next, the asymptotic behavior of the length of the canonical string is studied. Let  $\rho$  be the probability that an element of the adjacency matrix is 1, i.e., it is an active cell. It will be assumed that each cell is independent of all the others. The behavior for large sparse graphs is studied, i.e.  $N \rightarrow \infty$ ,  $\rho \rightarrow 0$ . The average Manhattan distance  $\delta$  from an active cell to the nearest active cell can be approximated by (see Appendix A):

$$\mathbb{E}[\delta] \sim \frac{\sqrt{\pi}}{2\sqrt{2}} \rho^{-1/2} \quad \text{as } N \rightarrow \infty, \rho \rightarrow 0 \quad (8)$$

The average number of instructions required to process an active cell may be approximated by  $\mathbb{E}[\delta] + 1$  because  $\delta$  pointer movement instructions must be executed, plus an  $E$  instruction. It must be highlighted that the actual number of instructions is higher because the closest other active cell may have been already processed by the algorithm. The average number of active cells in the adjacency matrix is  $N^2\rho$ . Therefore the length of the canonical string can be approximated by the product of both quantities:

$$\mathbb{E}[|I_G|] \sim \frac{\sqrt{\pi}}{2\sqrt{2}} N^2 \sqrt{\rho} \quad \text{as } N \rightarrow \infty, \rho \rightarrow 0 \quad (9)$$

where  $|\cdot|$  stands for the length of a string, and the term corresponding to the  $E$  instruction has been dropped because it becomes negligible in the limit. Equation (9) shows that for large, sparse graphs, the length of the canonical string  $I_G$  is much smaller than the length of the binary string representation which is  $N^2$ . Consequently, the proposed approach substantially compresses the structural information contained in the adjacency matrix, while it remains a reversible transformation.

### 2.3 Topological properties

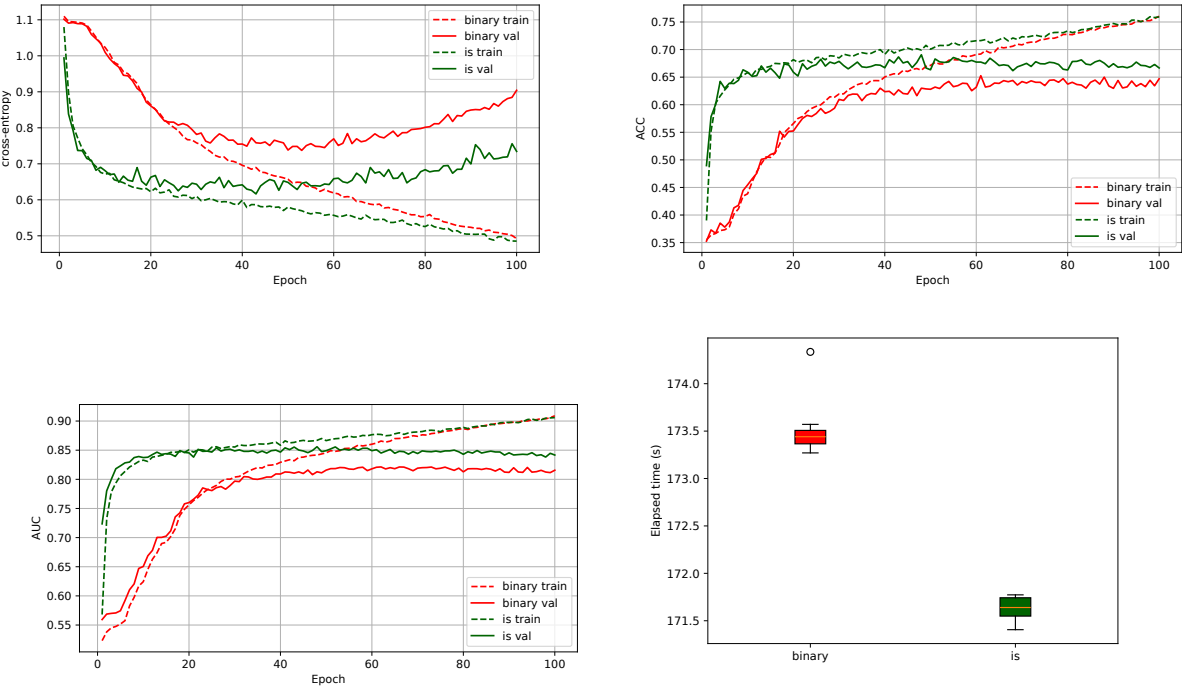
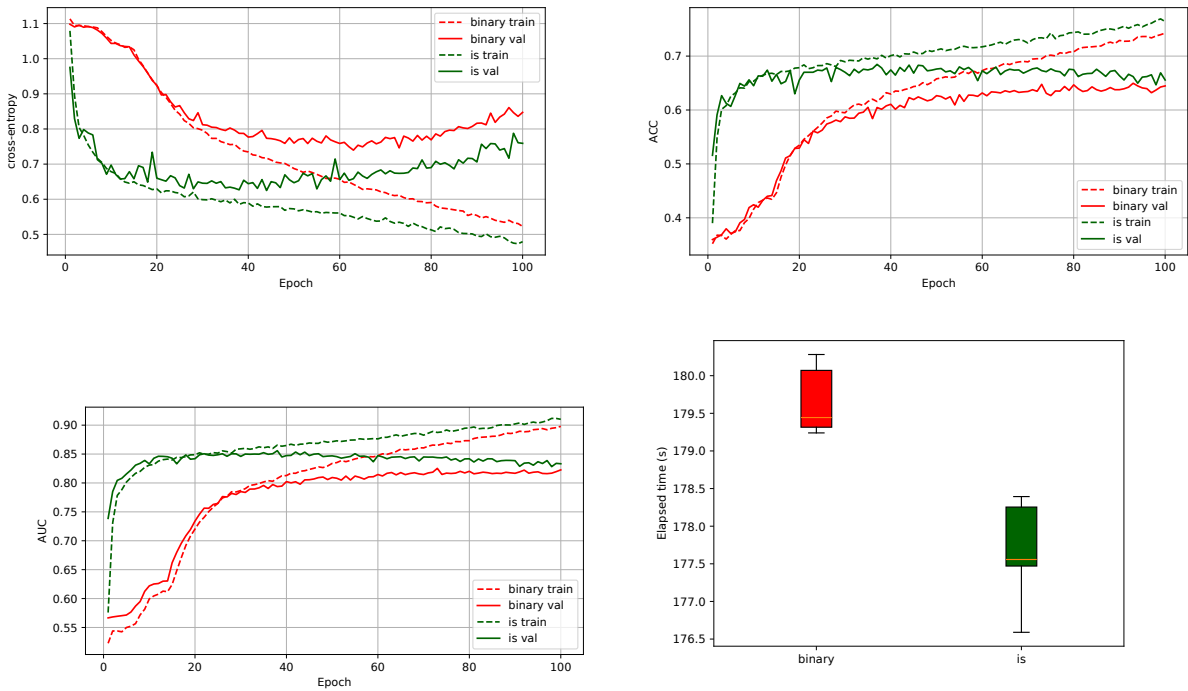
The proposed representation ensures that similar adjacency matrices are mapped to similar strings. This is a fundamental advantage for processing with deep learning models. Given an adjacency matrix  $M$ , an arbitrary cell  $(i, j)$ , and an instruction string  $w$  that represents  $M$ , let us consider the two cases that may arise when flipping the content of the cell:

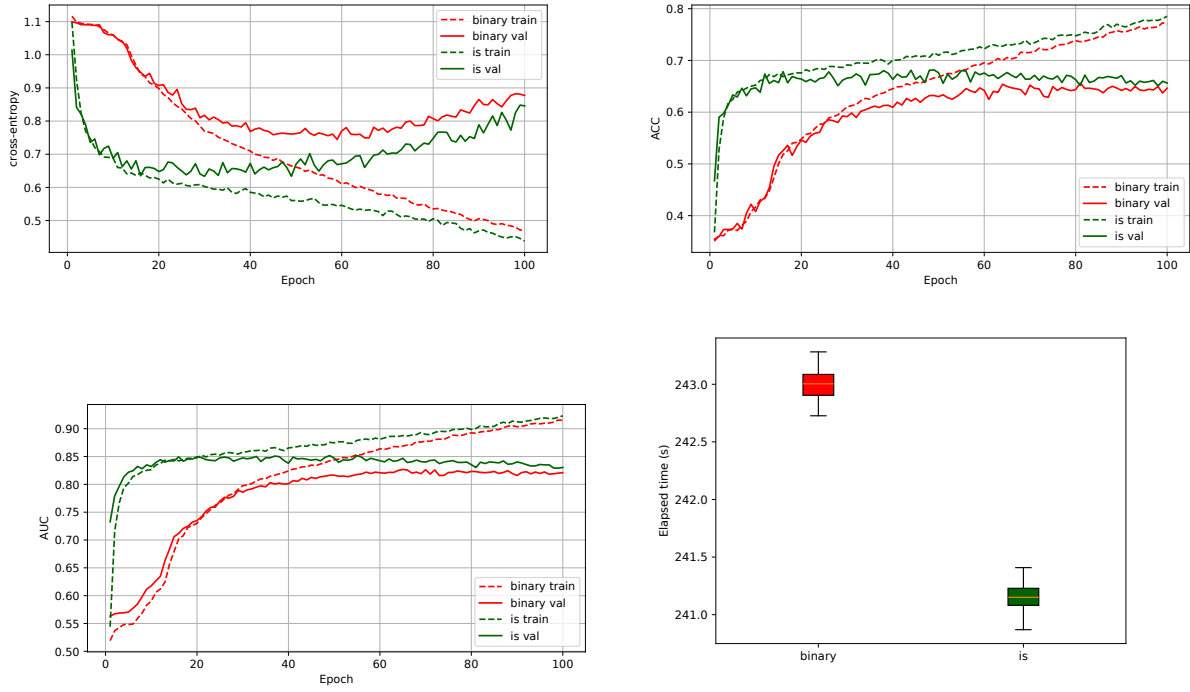
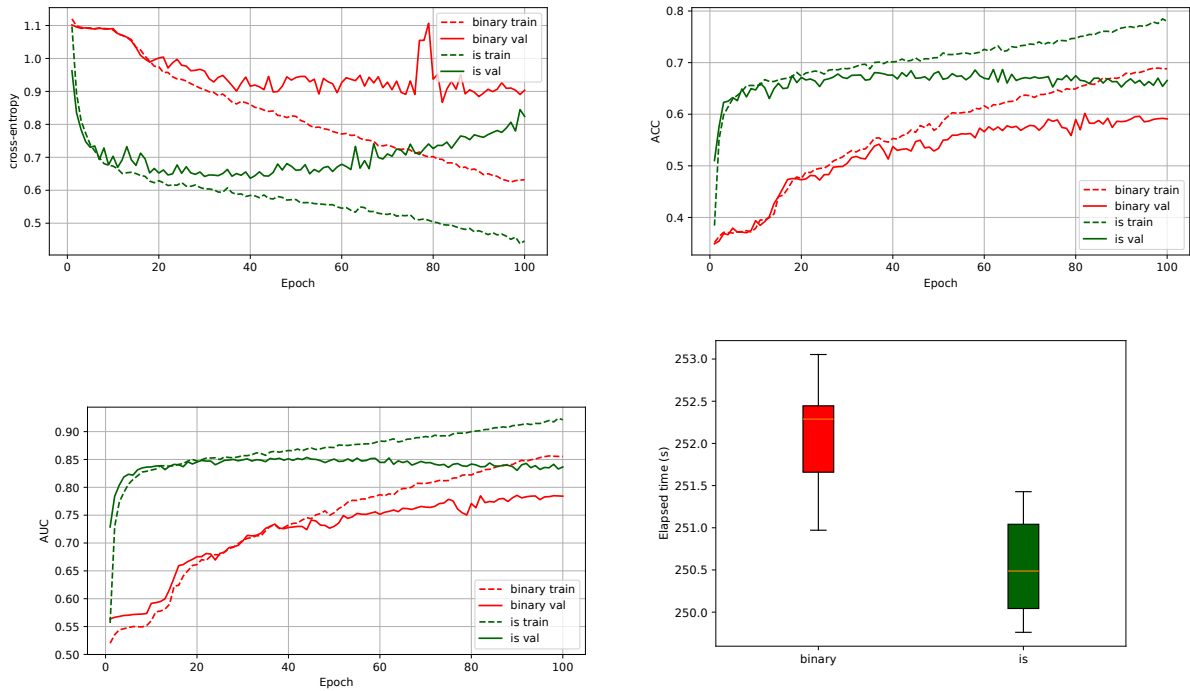
- If  $M(i, j) = 0$ , then the path formed by the cells that the pointer visits as  $w$  is executed may be considered. Let  $(i', j')$  be the cell within the path which is closest in Manhattan distance terms to  $(i, j)$ . Let  $\delta$  be such smallest Manhattan distance. Then a substring may be inserted in  $w$  at the point where  $(i', j')$  is visited. The substring moves the pointer from  $(i', j')$  to  $(i, j)$ , followed by an  $E$  instruction, and finally goes back to  $(i', j')$ . The inserted substring adds  $2\delta + 1$  instructions to the string length, and sets the element at  $(i, j)$  to 1, while leaving all the other elements with their previous values.
- If  $M(i, j) = 1$ , then there must be an  $E$  instruction in  $w$  that sets that element to 1. Let  $(i_{prev}, j_{prev})$  be the cell which is set to 1 by the previous  $E$  instruction, and  $(i_{next}, j_{next})$  be the cell which is set to 1 by the next  $E$  instruction. Consequently, the substring of  $w$  from the previous  $E$  instruction to the next  $E$  instruction may be substituted by a substring of movement instructions that take the pointer from  $(i_{prev}, j_{prev})$  to  $(i_{next}, j_{next})$  by the shortest path according to Manhattan distance. From the triangle inequality that Manhattan distance fulfills, it can be inferred that the new substring is no longer than the old one. Therefore, the overall string length cannot increase.

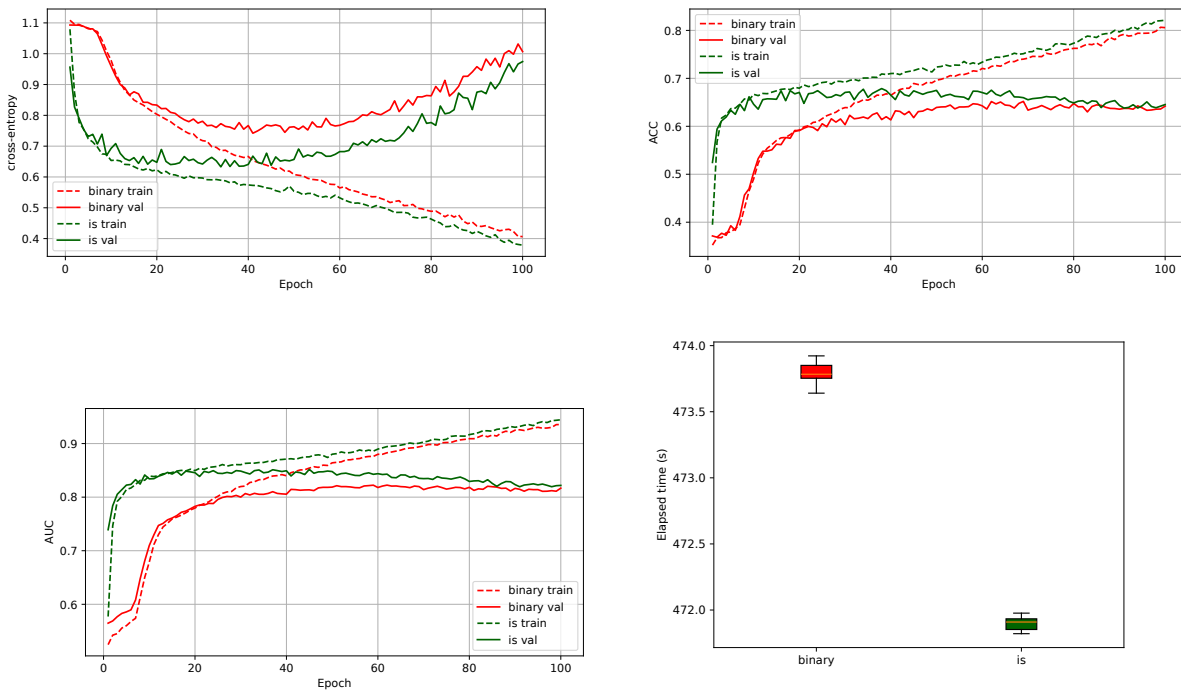
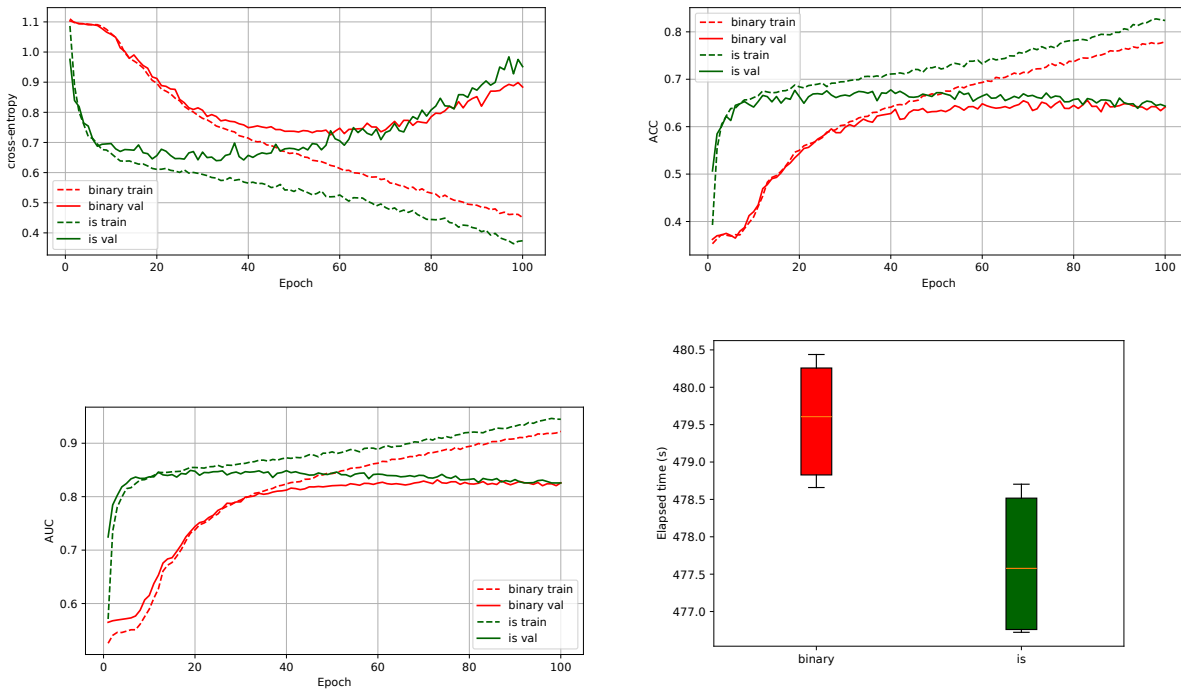
Together, the two above cases show that a minimal change in the adjacency matrix corresponds to a small modification in the representing string, as measured by the Levenshtein distance between strings. In other words, a local change in the graph structure is associated with a local change in the string. Therefore, local patterns in the graph are translated into substrings within the representing string.

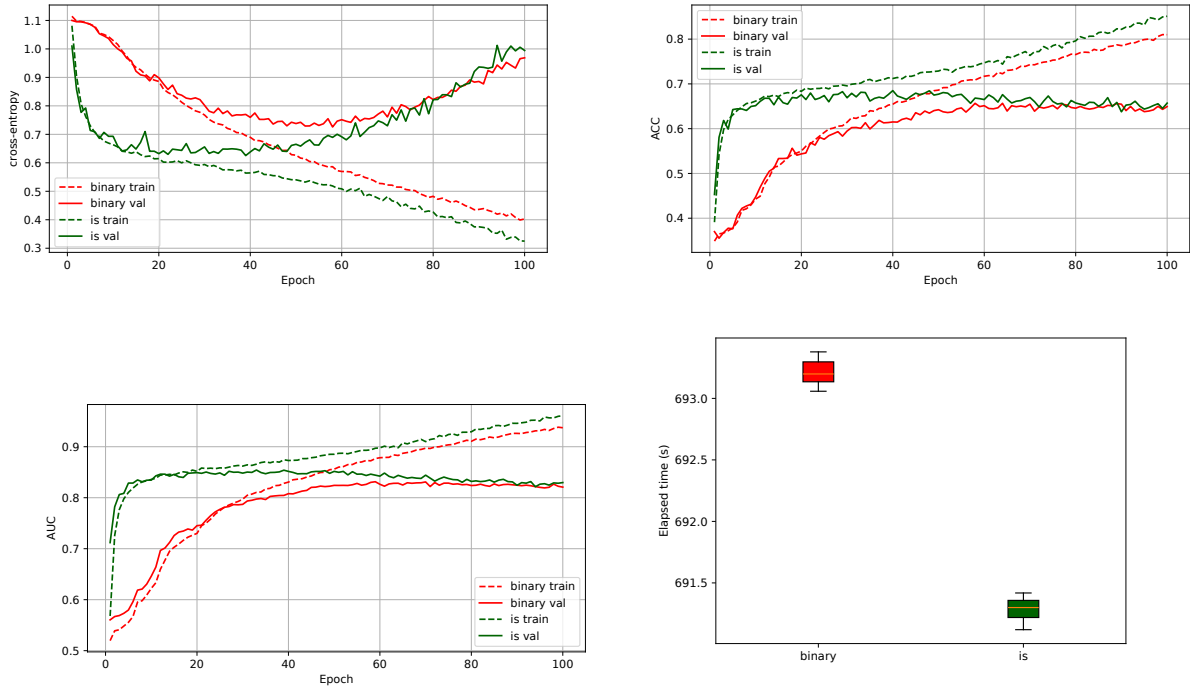
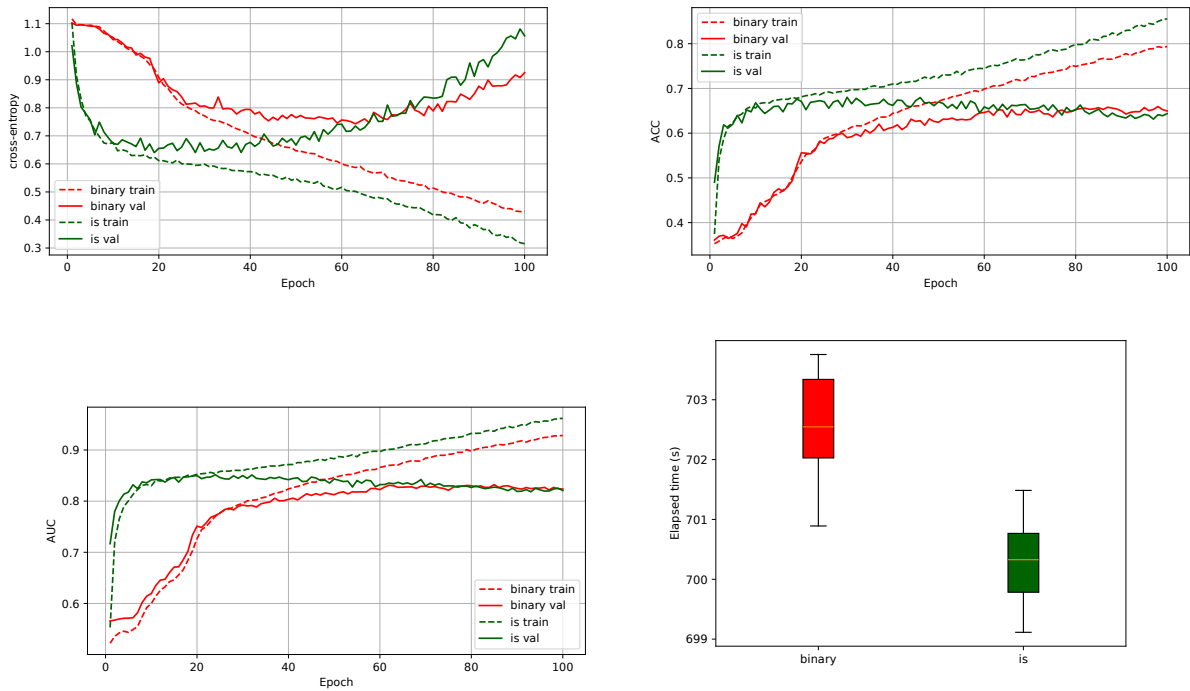
## 3 Computational experiments

In this section the results of some tentative experiments are reported. Subsection 3.1 explains how the synthetic dataset has been generated. Subsection 3.2 describes the neural transformer architectures that have been tested. After that, Subsection 3.3 details the experimental setup. Finally, Subsection 3.4 discusses the obtained results.

Figure 1: Results for the models with  $H = 4$ ,  $M = 2$ ,  $F = 128$ .Figure 2: Results for the models with  $H = 4$ ,  $M = 2$ ,  $F = 256$ .

Figure 3: Results for the models with  $H = 4$ ,  $M = 3$ ,  $F = 128$ .Figure 4: Results for the models with  $H = 4$ ,  $M = 3$ ,  $F = 256$ .

Figure 5: Results for the models with  $H = 16$ ,  $M = 2$ ,  $F = 128$ .Figure 6: Results for the models with  $H = 16$ ,  $M = 2$ ,  $F = 256$ .

Figure 7: Results for the models with  $H = 16$ ,  $M = 3$ ,  $F = 128$ .Figure 8: Results for the models with  $H = 16$ ,  $M = 3$ ,  $F = 256$ .

### 3.1 Dataset description

The synthetic dataset that has been tailored to test our approach is detailed next. A classification task has been designed, where three classes of undirected graphs must be recognized. Each graph represents adjacency relations in the three-dimensional space. A sequence of points in 3D space is defined for each graph. Each point is associated with a vertex of the graph. Then, an Euclidean distance threshold  $\zeta$  is established. Finally, the adjacency matrix of the graph contains an edge between each pair of vertices associated with points that are closer than the threshold  $\zeta$  in 3D space. Each class of graphs corresponds to a different way to generate a random sequence of points in 3D:

1. A single random walk whose length is  $2 + \psi$ , where  $\psi \sim \text{Poisson}(10)$ . Each step in the random walk is defined by a 3D displacement vector  $\mathbf{v} \in \mathbb{R}^3$  from the previous point, where  $\mathbf{v} \sim \text{Gauss}(\mathbf{0}, \mathbf{I})$ .
2. Two random walks, each with possibly different lengths  $1 + \psi_1, 1 + \psi_2$ , where  $\psi_1 \sim \text{Poisson}(5), \psi_2 \sim \text{Poisson}(5)$ . A step with a large displacement  $\mathbf{v} \sim \text{Gauss}(\mathbf{0}, 10 \cdot \mathbf{I})$  is taken between the two random walks.
3. A torus is considered with the following parametric equations:

$$x(\theta, \phi) = (K + k \cos \theta) \cos \phi \quad (10)$$

$$y(\theta, \phi) = (K + k \cos \theta) \sin \phi \quad (11)$$

$$z(\theta, \phi) = k \sin \theta \quad (12)$$

where  $K = 10$  is the major radius and  $k = 1$  is the minor radius. The length of the sequence is  $2 + \psi$ , where  $\psi \sim \text{Poisson}(10)$ . For the  $i$ -th point in the sequence,  $i \in \{0, 2, \dots, 1 + \psi\}$ , the first parameter  $\theta$  is set to  $\frac{2\pi(\xi+i)}{2+\psi}$ , where  $\xi \sim \text{Gauss}(0, 1)$ . This makes  $\theta$  span its entire range  $[0, 2\pi]$  with added Gaussian noise. The second parameter is set to  $\phi \sim \text{Uniform}(0, 2\pi)$ , which is a uniform random draw from its entire range of values.

For each class, the distance threshold  $\zeta$  is set to the 20th percentile of the distribution of distances, so that approximately 20% of the elements of each adjacency matrix are set to 1. This way, each class contains graphs that comprise different structures.

### 3.2 Description of the models

A range of simple neural transformer models has been selected in order to evaluate the advantages of the proposed graph representation methodology by instruction strings (*is*), as compared to the standard binary string representation (*binary*). Each transformer model processes an input string of characters and outputs three class scores associated with the three classes in the dataset. The architecture of the transformers comprises:

1. An input embedding layer.
2. A positional encoding layer.
3. A transformer encoder with  $M$  layers. Each layer has  $H$  heads, and a feedforward network model dimension  $F$ . The dropout is set to 0.1.
4. An output linear layer.

The embedding dimension is 64 for all layers except the linear layer. Eight model sizes have been tested, corresponding to  $M \in \{2, 3\}, H \in \{4, 16\}, F \in \{128, 256\}$ .

### 3.3 Experimental setup

A dataset of 3000 samples with 1000 samples per class has been drawn according to Subsection 3.1. The graphs of the dataset have been represented with binary strings (baseline) and instruction strings (our proposal). For each string representation and model size, a 10-fold cross-validation has been run. Four NVidia A100 GPUs with 40GB VRAM each have been employed for the experiments. The cross-entropy has been employed as the training loss. The Adam optimizer with learning rate 0.001 and batch size 64 has been chosen, with 100 training epochs.

Four performance metrics have been measured:

- The cross-entropy loss.
- The classification accuracy (*ACC*).
- The Area Under the Curve (*AUC*) following the One Versus Rest criterion.
- The overall computation time, including training and validation.

For each performance metric, the values for the 10 cross-validation folds have been collected. The means over the 10 folds on the training and validation sets have been computed for the first three metrics.

### 3.4 Results

In this subsection the results of the experiments are reported. Figures 1 to 8 depict the obtained results. The cross-entropy loss results indicate that the networks learn correctly for several tens of epochs. After that, the overfitting regime starts, in all cases well before the 100 epoch limit, marked by an increase in the validation set cross-entropy. Therefore, the overall behavior of the learning process is as expected. The models that use the instruction string representation tend to learn faster while they attain a better validation set cross-entropy, which demonstrates that learning is easier with our proposal.

These results are further confirmed by the downstream task metrics, namely the accuracy and the Area Under the Curve. Both metrics show that the instruction string representation consistently obtains the best classification performance. The models that run on the binary representation cannot reach the performance values of our proposal, no matter how long they are trained.

Regarding the computation time, our proposal is the fastest for all model sizes. The differences are not very significant, which may be due to the fact that the strings are not very long. More acute differences may be encountered for longer strings corresponding to larger graphs.

## 4 Conclusion

A new method to represent the structure of a graph by a sequence of instructions has been proposed. Each string in the regular language formed by all strings over an alphabet of five instructions represents a graph. Conversely, any graph can be represented by an infinite set of strings of such language. A canonical string is defined for each graph. Consequently, a reversible transformation between strings and graphs is defined. The representation is compact because a reduced number of instructions is needed to represent a graph, in particular for large, sparse graphs. Moreover, small changes in a graph correspond to small Levenshtein distances between the representing strings. Therefore, local changes remain local as the transformation is applied.

Together, all these properties suggest that the proposed representation is amenable for its use with deep learning models, in particular language models. Tentative experiments indicate that this may well be the case.

## Acknowledgment

The author thankfully acknowledges the computer resources (Picasso Supercomputer), technical expertise, and assistance provided by the SCBI (Supercomputing and Bioinformatics) center of the University of Málaga.

## Appendix A

For a large adjacency matrix with i.i.d. activations of density  $\rho \rightarrow 0$ , the mean Manhattan distance  $\delta$  from a typical active cell to its nearest other active cell scales like a constant times  $\rho^{-1/2}$ . More precisely, the asymptotic form is

$$\mathbb{E}[\delta] \sim C \rho^{-1/2}, \quad \rho \rightarrow 0,$$

with  $C$  of order 1.

For a continuum approximation by a homogeneous Poisson point process of intensity  $\lambda = \rho$  on  $\mathbb{R}^2$ , the number of other active cells inside the L1 ball of radius  $r$ ,

$$B_1(0, r) = \{x \in \mathbb{R}^2 : \|x\|_1 \leq r\},$$

is Poisson with mean  $\lambda \text{Area}(B_1(0, r)) = \lambda \cdot 2r^2$ .

Hence the survival function of the nearest–neighbor L1 distance  $S$  for a typical point is

$$\mathbb{P}(S > r) = \exp(-2\lambda r^2), \quad r \geq 0.$$

Differentiating gives the probability density

$$f_S(r) = 4\lambda r e^{-2\lambda r^2}, \quad r \geq 0.$$

The mean nearest–neighbor distance in this model is

$$\mathbb{E}[S] = \int_0^\infty r f_S(r) dr = 4\lambda \int_0^\infty r^2 e^{-2\lambda r^2} dr.$$

Evaluating the integral yields

$$\mathbb{E}[S] = \frac{\sqrt{\pi}}{2\sqrt{2}} \lambda^{-1/2} \approx 0.6267 \lambda^{-1/2}.$$

Identifying  $\lambda = \rho$  gives the asymptotics for the adjacency matrix model:

$$\mathbb{E}[\delta] \sim \frac{\sqrt{\pi}}{2\sqrt{2}} \rho^{-1/2} \quad \text{as } \rho \rightarrow 0.$$

## References

Jie Zhou, Ganqu Cui, Shengding Hu, Zhengyan Zhang, Cheng Yang, Zhiyuan Liu, Lifeng Wang, Changcheng Li, and Maosong Sun. Graph neural networks: A review of methods and applications. *AI Open*, 1:57–81, 2020. ISSN 2666-6510. doi:10.1016/j.aiopen.2021.01.001.

Shima Khosraftar and Aijun An. A survey on graph representation learning methods. *ACM Transactions on Intelligent Systems and Technology*, 15(2):1–45, 2024. doi:10.1145/3633518.

Weiyu Ju et al. A comprehensive survey on deep graph representation learning. *Neural Networks*, 171:1063–1095, 2024. doi:10.1016/j.neunet.2024.106207.

Bryan Perozzi, Rami Al-Rfou, and Steven Skiena. Deepwalk: Online learning of social representations. In *Proceedings of the 20th ACM SIGKDD International Conference on Knowledge Discovery and Data Mining*, pages 701–710. ACM, 2014. doi:10.1145/2623330.2623732.

Aditya Grover and Jure Leskovec. node2vec: Scalable feature learning for networks. In *Proceedings of the 22nd ACM SIGKDD International Conference on Knowledge Discovery and Data Mining*, pages 855–864. ACM, 2016. doi:10.1145/2939672.2939754.

Mikhail Belkin and Partha Niyogi. Laplacian eigenmaps for dimensionality reduction and data representation. *Neural Computation*, 15(6):1373–1396, 2003. doi:10.1162/089976603321780317.

Mingdong Ou, Peng Cui, Jian Pei, Ziwei Zhang, and Wenwu Zhu. Asymmetric transitivity preserving graph embedding. In *Proceedings of the 22nd ACM SIGKDD International Conference on Knowledge Discovery and Data Mining*, pages 1105–1114. ACM, 2016. doi:10.1145/2939672.2939751.

Quan Wang, Zhendong Mao, Bin Wang, and Li Guo. Knowledge graph embedding: A survey of approaches and applications. *IEEE Transactions on Knowledge and Data Engineering*, 29(12):2724–2743, 2017. doi:10.1109/TKDE.2017.2754499.

Zonghan Wu, Shirui Pan, Fengwen Chen, Guodong Long, Chengqi Zhang, and Philip S. Yu. A comprehensive survey on graph neural networks. *IEEE Transactions on Neural Networks and Learning Systems*, 32(1):4–24, 2021. doi:10.1109/TNNLS.2020.2978386.

Justin Gilmer, Samuel S. Schoenholz, Patrick F. Riley, Oriol Vinyals, and George E. Dahl. Neural message passing for quantum chemistry. In *Proceedings of the 34th International Conference on Machine Learning*, volume 70 of *Proceedings of Machine Learning Research*, pages 1263–1272. PMLR, 2017.

Thomas N. Kipf and Max Welling. Semi-supervised classification with graph convolutional networks. In *International Conference on Learning Representations*, 2017. arXiv:1609.02907.

William L. Hamilton, Rex Ying, and Jure Leskovec. Inductive representation learning on large graphs. In *Advances in Neural Information Processing Systems*, volume 30, pages 1024–1034, 2017.

Petar Veličković, Guillem Cucurull, Arantxa Casanova, Adriana Romero, Pietro Liò, and Yoshua Bengio. Graph attention networks. In *International Conference on Learning Representations*, 2018. arXiv:1710.10903.

Joan Bruna, Wojciech Zaremba, Arthur Szlam, and Yann LeCun. Spectral networks and locally connected networks on graphs. In *International Conference on Learning Representations*, 2014. arXiv:1312.6203.

Keyulu Xu, Weihua Hu, Jure Leskovec, and Stefanie Jegelka. How powerful are graph neural networks? In *International Conference on Learning Representations*, 2019. arXiv:1810.00826.